2022 4th International Conference on Sustainable Technologies for Industry 4.0 (STI), 17-18 December, Dhaka

Spherical and Rod-shaped Gold Nanoparticles for Surface Enhanced Raman Spectroscopy

Md. Shaha Alam[*†], Syed Farid Uddin Farhad[*§†], Nazmul Islam Tanvir[*§†], Md. Nur Amin Bitu[*§†], Mohammad Moniruzzaman[*†], Mahmuda Hakim[†], and Md. Aftab Ali Shaikh[†]
[*]Central Analytical and Research Facilities (CARF), Dhaka 1205, Bangladesh
[§]Energy Conversion and Storage Research, Industrial Physics Division, BCSIR Labs, Dhaka 1205, Bangladesh
[†]Bangladesh Council of Scientific and Industrial Research (BCSIR), Bangladesh
Email: shah.du.ch92@gmail.com , sf1878@bristol.ac.uk, nazmul.tanvir88@gmail.com, nabitu.ru@gmail.com, monirbcsir@gmail.com, mahmuda.silvi@yahoo.com, aftabshaikh@du.ac.bd,

2022 4th International Conference on Sustainable Technologies for Industry 4.0 (STI) | 978-1-6654-9045-0/22/$31.00 ©2022 IEEE | DOI: 10.1109/STI56238.2022.10103260

Abstract— **Raman Spectroscopy offers an in-situ, rapid, and non-destructive characterization tool for the chemical analysis of diverse samples with minimal or no preparation. However, due to the inherent weak signal of conventional Raman spectroscopy, surface plasmon resonance features of various nanostructures have been utilized to conduct Surface Enhanced Raman Spectroscopy (SERS) in detecting trace-level contaminants in foods and foodstuffs. In this effort, we synthesized gold nanoparticles (AuNPs) by reducing chloroauric acid ($HAuCl_4$) using sodium citrate dihydrate. We prepared different sizes of AuNPs at a fixed temperature (100 ºC) but with two different pHs, 4 and 8. UV-Vis spectroscopy, Dynamic Light Scattering (DLS), and Field Emission Scanning Electron Microscopy (FE-SEM) were used to analyze the synthesized AuNPs. FE-SEM micrographs revealed spherical AuNPs with an average diameter of ~55 ± 13 nm and rod-shaped AuNPs with an average length of ~170 ± 36 nm for samples synthesized at pH 8 and 4, respectively. The effectiveness of the as-prepared AuNPs for SERS is tested by detecting Rhodamine 6G (R6G) diluted at a trace level. This study suggests that plasmonic nanoparticles coupled with SERS have great potential for broad applications in detecting other trace amounts of hazardous elements in foods and foodstuffs.**

Keywords— ***Surface Enhanced Raman Spectroscopy (SERS), Rhodamine 6G, Gold nanoparticles, Liquid phase SERS***

I. Introduction

Raman spectroscopy is a simple but powerful characterization tool to determine the vibrational structure of molecules with minimal or no sample preparation [1-3]. Due to its non-destructive sample analysis nature, Raman spectroscopy has been widely used in many disciplines, including analytical chemistry [2, 3], materials science [4-8], food and agricultural industries ([3] and refs. therein), biological science [9, 10], as well as forensic and pharmaceutical science [11, 12]. However, due to the inherent weak signal of conventional Raman spectroscopy, surface plasmon resonance features of diverse nanostructures have been utilized to increase the strength of Raman signals. The latter procedure is called Surface Enhanced Raman Spectroscopy (SERS) [1-3, 13]. Among various nanomaterials, gold nanoparticles (AuNPs) draw significant attention from scientists in SERS measurements [9-14]. For SERS enhancement, the commercial substrates are expensive, and preparation methods are complicated and time-consuming. To address this issue, we synthesized different sizes and shapes of AuNPs using a facile technique; and further checked their utility by enhancing the Raman intensity of Rhodamine 6G (R6G) on stainless steel (SS) substrate. R6G is a cationic dye; toxic to living organisms; it provokes skin allergic reactions and is harmful to the respiratory tract, reproductive system, eyes, etc. [15]. Food and Drug Administration (FDA) banned its use in food additives; however, due to its low-cost many food industries use it as a food colorant [16-19]. Recently, Furong Tian *et al.* used gold nanospheres, nanotriangles, and nanostars to understand and optimize surface-enhanced Raman scattering [20]. Using nanostars, they found an enhancement (~6 times) of R6G Raman signals deposited on crystalline CaF_2 substrate, but no such significant enhancement in the case of the nanospheres. In this study, we prepared AuNPs of two different sizes and shapes (nanosphere and nanorod) to obtain the best SERS enhancement for detecting the R6G at a trace level. Plasmonic nanoparticle-assisted SERS techniques have the potential even to detect single molecules suggesting that SERS will be one of the best sustainable technologies aligned with Industry 4.0 to rapidly identify different inorganic, organic, and biological contaminants in foods and foodstuffs.

II. Experimental Section

A. Chemicals

Both auric chloride ($HAuCl_4$) and sodium citrate dihydrate with purity~99.9 % and ~99.0%, respectively, were procured from Sigma-Aldrich and utilized without additional purification. Nitric acid and hydrochloric acid were purchased from Fisher Scientific and certified ACS Plus. All solution preparation procedures were conducted by utilizing highly pure (18.2 MΩ-cm) deionized (DI) water.

B. Preparation of gold nanoparticles

In a typical procedure of AuNPs, 30.0 mL of 19.4 mM sodium citrate dihydrate solution (adjusted pH at 8.0 by adding 5 M NaOH) and a magnetic stir bar were added to a three-angled neck flask. This flask was set on a hotplate and coupled with a condenser. This condenser was placed on the center neck, with a thermometer and a glass stopper on the two other sides of the neck. The solution was boiled for 20 min at 100 ^{0}C, and then freshly prepared 1.0 mL of 1 mM $HAuCl_4$ solution was added. Until the appearance of wine-red color, the reaction was allowed to proceed. The gold nanoparticles (AuNPs) formation can be inferred by observing the wine-red solution color. The same procedure was also followed at pH 4 (adjusted by adding 5 M HCl) for 10 mM sodium citrate dihydrate solution and 5 mM $HAuCl_4$ to control the morphology and size of the resulting AuNPs (solution color was violet). The graphical presentation of the whole synthesis procedure is shown in Fig. 1.

978-1-6654-9045-0/22/$31.00 ©2022 IEEE

Fig. 1. Synthesis procedure of gold nanoparticles (AuNPs)

C. Characterizations and Instrumentations

The absorption spectra of different AuNPs were recorded at room temperature (~25 °C) using Shimadzu 2600 UV-VIS-NIR spectrometer. The maximum absorption peak in the spectrum was used to determine the surface plasmon resonance (SPR) wavelength (λ_{max}) of the synthesized AuNPs. Dynamic Light Scattering (DLS) (Horiba SZ-100V2) has been employed to estimate the average particle size (APS), and zeta potential of gold nanoparticle solution. The surface morphology of the AuNPs was investigated by a Field Emission-Scanning Electron Microscope (FE-SEM, JOEL 7610F). SERS studies of AuNPs coupled with R6G were recorded at room temperature using a Raman spectrometer (Horiba MacroRam) with a diode laser having a peak wavelength of 785 nm. The laser power was kept below 5 mW at the sample surface to prevent sample degradation.

III. Results And Discussion

The color change in the reaction solution from pale yellow to wine red (Fig. 1) indicates that the AuNPs formation is completed, and one can easily spot the difference in color change. The sodium citrate functions as a stabilizing agent, a capping agent, and a reducing agent to turn Au^{3+} ion to Au^{0}. Intriguingly, violet and red-wine AuNPs solutions were found at pH 4 and 8 of the precursors.

Fig. 2(a, b) and their respective inset represent the UV–Vis spectra of as-synthesized AuNPs and solution color. Interestingly, AuNPs are seen to have a specific Surface Plasmon Resonance (SPR) band between 450 to 600 nm, red-wine AuNPs solution with $\lambda_{max} \approx 534$ nm (Fig. 2a), and violet AuNPs solution with $\lambda_{max} \approx 542$ nm (Fig. 2b) due to the variation in shape and size of the nanoparticles in the solutions. Larger particles underwent increased scattering and had a resonance peak that broadened significantly and shifted towards longer wavelengths (known as red-shift). This was further confirmed by the DLS measurements: APS $\approx$ 50 nm for $\lambda_{max} \approx 534$ nm AuNPs solution and APS $\approx$ 193 nm for $\lambda_{max} \approx 542$ nm AuNPs solution shown in Fig. 3. The smaller AuNPs solution was found to have zeta potential (mean) is –34.4 mV compared to –12.9 mV for larger AuNPs solution. These UV-Vis and DLS observations corroborate reported studies by others [21-23].

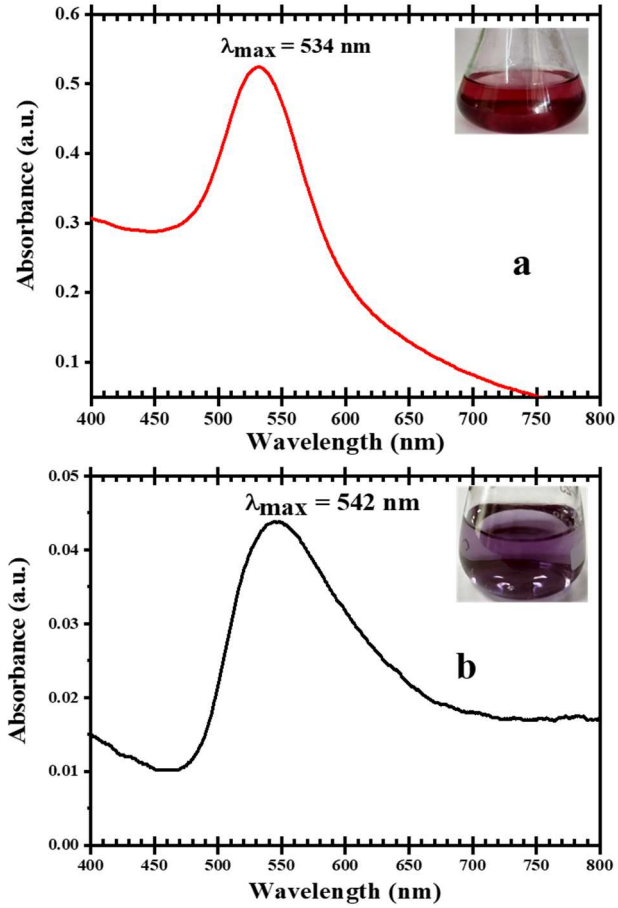

Fig. 2. UV-Vis spectra of as-synthesized AuNPs

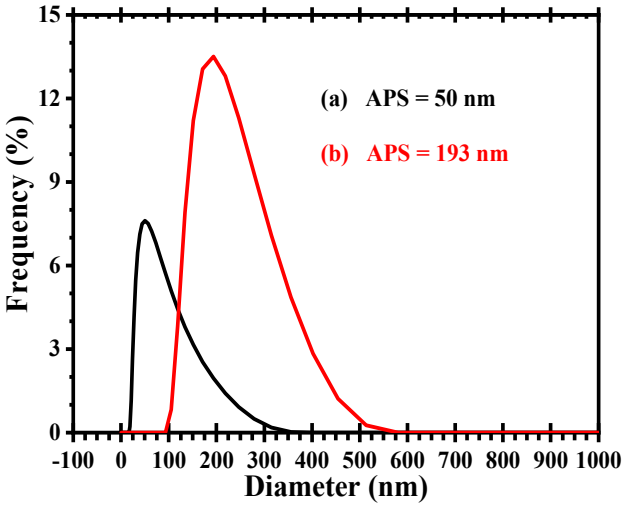

Fig. 3. DLS graph shows the average particle size (APS) and distribution of AuNPs synthesized under two different conditions.

The size and shape of AuNPs may affect the SERS enhancement of samples under investigation [24, 25]. The morphology of AuNPs affects their attachment to the sample under study (e.g., R6G). To this end, FE-SEM micrographs of AuNPs grown at pH 8 and pH 4 of precursor solution were analyzed by ImageJ software [7], and the results are displayed with the respective image in Fig. 4.

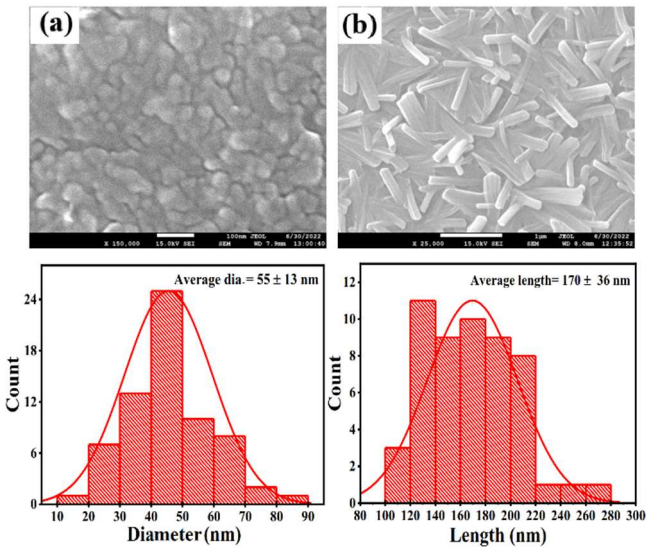

Fig. 4: SEM Micrographs and size distribution curve of (a) spherical and (b) nanorod-shaped AuNPs

As can be seen from Fig. 4, FE-SEM images revealed almost spherical-shaped AuNPs with a mean diameter of ~55 ± 13 nm for red-wine solution (Fig. 4a) and rod-shaped AuNPs with a mean length of ~170 ± 36 nm (Aspect ratio ~5.15; dia. ~34 ± 8 nm; size distribution data are not shown here) for violet-solution. Indeed, the FE-SEM analyzed size measurements of AuNPs corroborate the DLS-derived size measurements within the error margin.

SERS spectra of Rhodamine 6G (R6G)

To elucidate the effect of spherical and rod-shaped AuNPs on the vibrational structure of R6G (0.2 mM), the SERS event of R6G adsorbed on colloidal AuNPs was studied in the region of 180-2000 cm^{-1}. These samples were prepared by drop casting of 5-10 µL AuNPs on R6G droplets on the stainless steel (SS) substrates, and then Raman spectra were recorded immediately on the liquid phase sample (without drying). For comparison purposes, the Raman signature of bare SS substrate, AuNPs, and R6G were also recorded under the same conditions and displayed in Fig. 5. From this figure, one can see that bare SS (Fig.5a), AuNPs on SS (Fig. 5b), and R6G on SS (Fig. 5c) did not exhibit any sharp Raman peaks in the range of 500-1800 cm^{-1}, except a broad hump near ~1400 cm^{-1}. In the case of the 'AuNPs on SS' sample, the vibration peak near 250 cm^{-1} was presumably induced from the plasmonic features of AuNPs, which is absent in bare SS, and R6G on SS but present again in AuNP (~55 nm (FE-SEM)) on R6G (Fig. 5d) and AuNP (~170 nm (FE-SEM)) on R6G (Fig. 5e) samples. Intriguingly, ~55 nm AuNPs (spherical) coupled R6G produced significant SERS enhancement compared to that of ~170 nm AuNPs (rod-shaped) associated R6G sample (cf. Fig. 5d and Fig. 5e). The SERS enhanced Raman peaks of R6G are in good agreement with our previous report done in solid phase sample [26].

Size and shape effect of AuNPs on SERS enhancement

The electromagnetic field of the incident laser beam is dramatically enhanced due to the resonant interaction with the free electrons of metal nanoparticles, called surface plasmon resonance (SPR). This enhanced electromagnetic field plays a pivotal role in the Raman signals of the molecules adjacent to the nanoparticle surface.

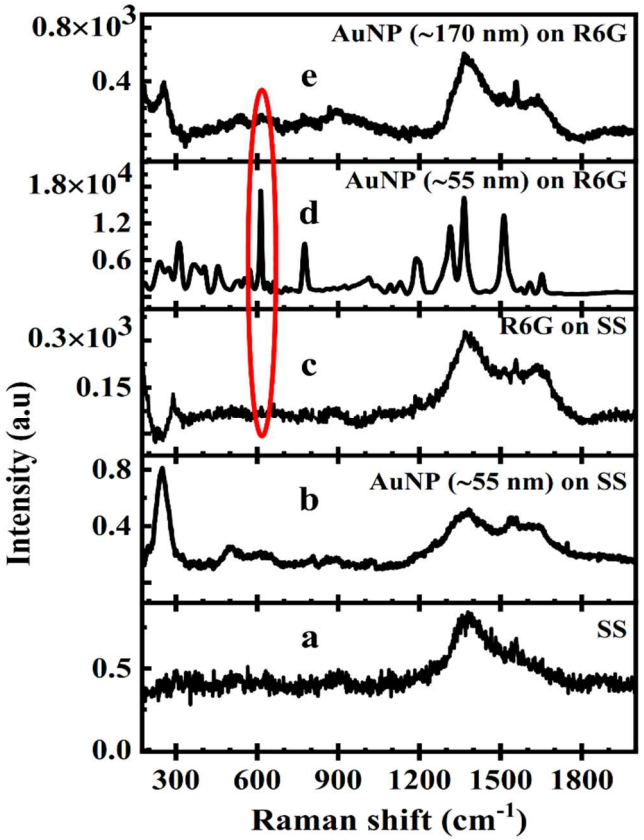

Fig. 5: Raman spectrum of (a) stainless steel substrate (SS), (b) AuNP on SS, (c) R6G on SS, (d, e) AuNP on R6G.

Nanoparticle size, shape, and degree of their aggregation affect the SERS enhancement [27]. Spherical-shaped and smaller-size (~55 nm) AuNPs exhibited the highest SERS enhancement (for example, the vibrational peak of R6G near 615 cm^{-1} enhanced ~18,000 times (see red-circled peaks in Fig. 5) compared to rod-shaped larger-size (~170 nm) AuNPs corroborating the reported results (dia. ~75 nm) [28]. The rod-shaped nanoparticles did not show significant enhancement, presumably due to the large aspect ratio (~5.15) and the absence of plasmonic bands at ~600 nm to 750 nm [29] near the excitation source. The present study was conducted using dilute 0.2 mM R6G, indicating that plasmonic nanoparticles coupled with SERS have great potential for use in diverse applications, for example, the detection of trace amounts of different hazardous chemicals in foods and foodstuffs. Further investigation of different sizes and shapes of AuNPs is currently in progress to elucidate the critical plasmonic size of AuNPs for detecting trace levels of pesticides added to food and agricultural products.

IV. Conclusion

This report describes a facile technique to synthesize size and shape-controlled AuNPs by controlling the pH and concentration of precursor solutions. As-synthesized gold nanoparticles were examined by a variety of characterization tools, including UV-Vis Spectroscopy, DLS, and FE-SEM, to elucidate their size and shape effect on the SERS activity of diluted R6G. Spherical AuNPs (~55 nm) exhibited excellent

SERS enhancement (~18,000 times) compared to nanorod-shaped AuNPs. This study also summarizes a simple, sensitive, and rapid approach to detecting hazardous chemicals in foods and foodstuffs, even at trace levels. This may enable us to find a sustainable technology to ensure food safety and environmental protection.

ACKNOWLEDGMENT

All the authors are thankful to the Industrial Physics Division (IPD), BCSIR Laboratories, Dhaka 1205, Bangladesh Council of Scientific and Industrial Research (BCSIR) and extend their appreciation for financial and logistic support under the scope of R&D project# TCS-FY2017-2022, Special Allocation Grant# 404-ES-FY2021-22 (Ref.# 39.00.0000.009.14.019.21-745 Dated 15/12/2021), Ministry of Science and Technology, Government of Bangladesh, the World Academy of Sciences (TWAS) Grant#20-143 RG/PHYS/AS_I, and Royal Society of Chemistry, UK Grant# R20-3167 for Energy Conversion and Storage Research (ECSR) Section of IPD.

REFERENCES

[1] F. Siebert, and P. Hildebrandt, "Theory of Infrared Absorption and Raman Spectroscopy," Vibrational Spectroscopy in Life Science, pp. 11-61, 2008.

[2] K. M. Abedin, S. F. U. Farhad, M. R. Islam, A. I. Talukder, and A. F. M. Y. Haider, "Construction and operation of a dispersive laser Raman spectrograph using interference filter," J. Bangladesh Acad. Sci., vol. 32, pp. 121-129, 2008.

[3] S. F. U. Farhad, K. M. Abedin, M. R. Islam, A. I. Talukder, and A. F. M. Y. Haider, "Determination of ratio of unsaturated to total fatty acids in edible oils by laser Raman spectroscopy," Res. J. Appl. Sci., vol. 9, pp. 1538-1543, 2009.

[4] M. R. Islam, M. Saiduzzaman, S. S. Nishat, A. Kabir, and S. F. U. Farhad, "Synthesis, characterization and visible light-responsive photocatalysis properties of Ce doped CuO nanoparticles: A combined experimental and DFT+U study," Colloids Surf, A Physicochem Eng Asp., vol. 617, 126386, 2021.

[5] A. M. M. Musa, S. F. U. Farhad, M. A. Gafur, and A. T. M. K. Jamil, "Effects of withdrawal speed on the structural, morphological, electrical, and optical properties of CuO thin films synthesized by dip-coating for CO_2 gas sensing," AIP Advances, vol. 24, pp. 401–409, 2021.

[6] B. C. Ghos, S. F. U. Farhad, M. A. M. Patwary, S. Majumder, M. A. Hossain, N. I. Tanvir, M. A. Rahman, T. Tanaka, and Q. Guo, "Influence of the substrate, process conditions, and post-annealing temperature on the properties of ZnO thin films grown by the successive ionic layer adsorption and reaction method," ACS Omega, vol. 6, pp. 2665−2674, 2021.

[7] S. F. U. Farhad, R. F. Webster, and D. Cherns, "Electron microscopy and diffraction studies of pulsed laser deposited cuprous oxide thin films grown at low substrate temperatures," Materialia, vol. 3, pp. 230-238, 2018.

[8] M. R. Molla, M. H. A. Begum, S.F.U. Farhad, A. S. M. A. Rahman, N. I. Tanvir, M. S. Bashar, R. H. Bhuiyan, M. S. Alam, M. S. Hossain, and M. T. Rahman, "Facile extraction and characterization of calcium hydroxide from paper mill waste sludge of Bangladesh," R. Soc. Open Sci. vol. 9, issue 8, 220681, 2022.

[9] Q. Tu, C. Chang, "Diagnostic applications of Raman spectroscopy" Nanomed.: Nanotechnol. Biol. Med., vol. 8, pp. 545-558, 5, 2012.

[10] K. Dodo, K. Fujita, and M. Sodeoka, "Raman spectroscopy for chemical biology research" J. Am. Chem. Soc, vol. 144, 43, pp. 19651–19667, 2022.

[11] V. Bijuab, "Chemical modifications and bioconjugate reactions of nanomaterials for sensing, imaging, drug delivery and therapy," Chem. Soc. Rev., vol. 43, pp. 744-764, 2014.

[12] L. Thobakgale, S. O. Lemboumba, and P. M. Kufa, "Chemical sensor nanotechnology in pharmaceutical drug research," Nanomaterials, vol. 12, 2688, 2022.

[13] X. X. Han, R. S. Rodriguez, C. L. Haynes, Y. Ozaki, and B. Zaho, "Surface-enhanced Raman spectroscopy," *Nat Rev Methods Primers* 1, vol. 87, 2021.

[14] K. Nejati, M. Dadashpour, T. Gharibi, H. Mellatyar, and A. Akbarzadeh, "Biomedical applications of functionalized gold nanoparticles: A review," J. Clust. Sci, vol. 33, pp. 1–16, 2022.

[15] Rhodamine 6G Solution MSDS "Pioneer Forensics - PF045," 14 June 2013.

[16] N. Xiao, J. Deng, K. Huang, S. Ju, C. Hu, and J. Liang, "Application of derivative and derivative ratio spectrophotometry to simultaneous trace determination of rhodamine B and rhodamine 6G after dispersive liquid-liquid microextraction," Spectrochim. Acta A Mol. Biomol. Spectrosc., vol. 128, pp. 312-318, 2014.

[17] J. Wang, J. Li, C. Zeng, Q. Qu, M. Wang, W. Qi, R. Su, and Z. He, "Sandwich-like sensor for the highly specific and reproducible detection of Rhodamine 6G on a surface-enhanced Raman scattering platform," ACS Appl. Mater. Interfaces, vol. 12, pp. 4699-4706, 2020.

[18] K. Sridhar, B. S. Inbaraj, and B. H. Chen, "An improved surface-enhanced Raman spectroscopic method using a paper-based grape skin-gold nanoparticles/graphene oxide substrate for detection of rhodamine 6G in water and food," Chemosphere, vol. 301, 134702, 2022.

[19] A. Dhawan, Y. Du, F. Yan, M. D. Gerhold, V. Misra, and T. Vo-Dinh, "Methodologies for developing Surface Enhanced Raman Scattering (SERS) substrates for the detection of chemical and biological molecules," IEEE Sensors Journal, vol. 10, pp. 608-616, 2010.

[20] F. Tian, F. Bonnier, A. Casey, A. E. Shanahan, and H. J. Byrne, "Surface Enhanced Raman Scattering with gold nanoparticles: Effect of particle shape," Anal. Methods, vol. 6, pp. 9116-9123, 2014.

[21] L. Yang, Z. Wei, R. Tayebee, E. Koushki, and H. Bai, "Effects of laser penetration depth and temperature on the stability of afatinib-loaded gold nanoparticles: an optical limiting study," J. Nanoparticle Res., vol. 24, 2022.

[22] Y. Xu, F. Y. H. Kutsanedzie, M. Hassan, J. Zhu, W. Ahmad, H. Li, and Q. Chen, "Mesoporous silica supported orderly-spaced gold nanoparticles SERS-based sensor for pesticides detection in food," Food Chem., Vol. 315, 126300, 2020.

[23] Y. Zhuang, L. Liu, X. Wu, Y. Tian, X. Zhou, S. Xu, Z. Xie, and Y. Ma, "Size and shape effect of gold nanoparticles in "Far-Field" Surface Plasmon Resonance." Part. Part. Syst. Charact., vol. 36, 1800077, 2018.

[24] A. Chakraborty, A. Das, S. Raha, and A. Barui, "Size-dependent apoptotic activity of gold nanoparticles on osteosarcoma cells correlated with SERS signal," J. Photochem. Photobiol. B, Biol., vol. 203, 111778, 2020.

[25] A. I. L. Lorente "Recent developments on gold nanostructures for surface-enhanced Raman spectroscopy: Particle shape, substrates, and analytical applications. A review," Analytica Chimica Acta, vol. 1168, 338474, 2021.

[26] A. Islam, F. Tasneem, Z. H. Khan, A. Rakib, S. F. U. Farhad, A. I. Talukder, A. F. M. Yusuf Haider, and M. Wahadoszamen, "Economically reproducible surface-enhanced Raman spectroscopy of different compounds in thin film," J. Bangladesh Acad. Sci., vol. 45, pp. 1-11, 2021.

[27] S. C. Boca, C. Farcau, and S. Astilean, "The study of Raman enhancement efficiency as a function of nanoparticle size and shape," Nuc. Inst. & Met. Phys. Res., Section B: Beam Interactions with Materials and Atoms, vol. 267, pp. 406-410, 2009.

[28] C. Zhai, Y. Y. Li, Y. K. Peng, and T. F. Xu, "Detection of chlorpyrifos in apples using gold nanoparticles based on surface-enhanced Raman spectroscopy," Int. J. Agri. & Biol. Eng., vol. 8, pp. 113-120, 2015.

[29] S. Yun, M. K. Oh, S. K. Kim, and S. Park, "Linker-molecule-free gold nanorod films: Effect of nanorod size on surface-enhanced Raman scattering," J. Phys. Chem. C, vol. 113, pp 13551-13557, 2009.